18th International Conference on Information Fusion
Washington, DC - July 6-9, 2015

An Evaluation of Monte Carlo for Nonlinear Initial Uncertainty Propagation in Keplerian Mechanics

Chao Yang[1], Kevin Buck[2] and Mrinal Kumar[3]

Abstract— **This paper evaluates the performance of traditional Monte Carlo (FMC) for the nonlinear propagation of initial uncertainty in the two-body problem: an essential task in space situational awareness. This is done in light of a newly developed Markov chain Monte Carlo (MCMC) based particle approach that combines the benefits of MCMC sampling with the method of characteristics (MOC) for solving first order partial differential equations - in this case, the stochastic Liouville equation (SLE). The resulting MCMC-MOC ensemble is by construction, equivalent in measure to the true state probability density. Our recent results on the MCMC-MOC approach indicate that for systems with divergence-free dynamics, the FMC and MCMC-MOC ensembles are statistically consistent. Unfortunately, the unperturbed two-body problem (Keplerian motion) is one such system. In this paper, we demonstrate through simulation that the traditional MC propagated ensemble is indeed equivalent in measure to MCMC-MOC ensemble, which in turn is the true system measure by construction. As a result, it is not possible to improve upon FMC and its slow convergence rate for this problem.**

I. INTRODUCTION

Space situational awareness (SSA) of Earth-orbiting resident space objects (RSOs), including active satellites and space debris, is known to be a "data starved" problem in that due to the stress on tracking resources, objects may not be observed for days if not weeks. Thus, accurate characterization of uncertainty associated with these objects is crucial for maintaining the space surveillance network (SSN) catalog, and ultimately making high impact decisions related to evaluation of collision risks, reacquiring objects from tracking stations and identification of previously untracked objects in the SSN catalog. Due to the ever-increasing number of RSOs and the concomitant sparsity of observational data, there is an increasing demand for improved uncertainty characterization and propagation for long periods of time. Additionally, accurate representation of the propagated uncertainty such as information about the higher moments leads to more accurate conjunction assessment and track correlation capabilities. To address these issues, several methods, including Monte-Carlo simulations [1], [2], Gaussian mixtures [3], [4], [5], spectral expansions [6], [7], and *direct* Fokker Planck equation (FPE) solvers [8], [9], [10] have been used.

The focus of this paper is on the particle paradigm for uncertainty forecasting. For initial uncertainty propagation, the most prevalent particle approach is the so-called Monte Carlo technique. Here, a large number of samples are randomly drawn from the initial state-pdf, thereby achieving a discretization. Each particle is then simply propagated forward in time through the system dynamics, causing a rearrangement of the samples. The desired statistics at any time is computed from the current configuration of the ensemble. While this approach is simple to implement, it faces several issues: (i) it is not clear how many particles are sufficient to accurately characterize the true nature of uncertainty in the state, (ii) occurrence of particle degeneracy resulting from their traversal to the tail regions as time moves forward, especially if the underlying system does not admit any stationary solutions or contains regions of instability in its state-space [11]. Essentially, it is not clear how well the propagated particles represent the uncertainty in the system at future times after discretization of the initial pdf. These issues are somewhat controversial and no definitive resolution is available in the current literature.

Recently, a new particle approach was introduced for solving the SLE [12], combining the Markov chain Monte Carlo (MCMC) sampling algorithm [13], [14] with the method of characteristics (MOC) [15]. In this approach, at any desired time, a Markov chain is constructed using the unknown state pdf as the target density. To evaluate the unknown target at a candidate sample, the SLE is solved via MOC. MOC requires the existence of a mapping between the current state and its corresponding initial condition, which is obtained numerically by back-propagating the candidate through the system dynamics along a characteristic curve. Then, the SLE is forward propagated along the same characteristic curve to obtain the value of the target density at the candidate sample. Metropolis acceptance criterion finally decides whether or not the candidate must be admitted into the particle representation of the state-pdf at the current time. This approach has several advantages: (i) MCMC does not require the specification of a domain: the Markov chain automatically samples more particles from regions where the probability mass is high, and (ii) the number of particles required is small because the samples are located only where they are needed, and more importantly, they are equivalent in measure to the current state pdf. Accordingly, they can be used directly to compute desired expectations of the state.

Typically, a "sufficiently large" FMC ensemble is employed as the benchmark particle representation of uncertainty. Of

*This work was supported by the National Science Foundation under Grant No. ECCS-1254244.

[1]Chao Yang is a graduate student in the Department of Mechanical Engineering, University of Florida, Gainesville, USA nanjinchaochao@ufl.edu

[2]Kevin Buck is an undergraduate in the Department of Aerospace Engineering, University of Florida, Gainesville, USA k.buck@ufl.edu

[3]Mrinal Kumar is an assistant professor in the Department of Mechanical and Aerospace Engineering, University of Florida, Gainesville, USA mrinalkumar@ufl.edu

course, there are no clear guidelines except apparent convergence of statistics to determine how large the ensemble must be. On the other hand, the MCMC-MOC ensemble is, by construction equivalent in measure to the true state-pdf. Our recent results have shown that for initial uncertainty forecasting, the MCMC-MOC and FMC ensembles are statistically equivalent if the underlying forcefield is divergence free ($\nabla \cdot \mathbf{f} = 0$). The unperturbed two-body problem (TBP) is one such system (with trivial divergence), and as a result, the current paper presents a "negative result" in the sense that despite the shortcomings of FMC (in particular, its slow convergence), it is not possible to find a better particle representation for the TBP.

The remainder of this paper is organized as follows: Section II presents the equation of motion of the two body system and its universal $F-G$ solution. Sections III and IV illustrate in detail the algorithms of FMC and MCMC-MOC. Then, numerical simulations are shown in Section V that demonstrate the statistical equivalence of the two methods. Section VI contains a summary of this study.

II. Two-Body Problem (TBP)

The two-body problem concerns the motion of two point masses that interact only with each other through the force of gravity, e.g. a satellite orbiting a planet or a binary star system. In this section, the dynamics of the two body problem and its so-called *universal $F-G$ solution* is briefly reviewed.

A. Problem Statement

We consider the following deterministic nonlinear dynamical system for the initial uncertainty propagation problem,

$$\dot{\mathbf{x}} = \mathbf{f}(t, \mathbf{x}), \; W(t_0, \mathbf{x}) = W_0(\mathbf{x}), \tag{1}$$

where, $\mathbf{x} \in \Re^N$ is the state of the dynamical system, the vector function $\mathbf{f}(t, \mathbf{x}) : [0, \infty) \times \Re^N \to \Re^N$ is the system dynamics and $W_0(\mathbf{x})$ is the initial probability density function (pdf). In the current paper, we are interested in the unperturbed Keplerian dynamics with uncertainty in initial conditions, described below.

B. Equations of Motion of the Two Body Problem

The fundamental equation of relative motion in the TBP is given by [16]:

$$\ddot{\mathbf{r}} = -\frac{\mu}{r^3}\mathbf{r}, \tag{2}$$

where, μ is the gravitational constant of the central object, $\mathbf{r}$ is the relative radius vector joining the two point masses ($\mathbf{r} \in \Re^3$), $r = \sqrt{r_1^2 + r_2^2 + r_3^2}$ is the magnitude of the radius vector and $\dot{\mathbf{r}} = \mathbf{v}$ is the velocity vector ($\mathbf{v} \in \Re^3$). The initial uncertainty is given by the probability density function (pdf) $W_0(\mathbf{x})$, where $\mathbf{x} \doteq [\mathbf{r}; \mathbf{v}]$. In the 3D Euclidean space, Eq.2 is a set of three second-order, or equivalently, six first-order coupled nonlinear ordinary differential equations (ODEs).

C. Universal $F-G$ Solution

A closed form solution of Eq.2 for $\mathbf{r}(t)$ and $\mathbf{v}(t)$ is not known. Here, we employ the so-called *Universal $F-G$ Solution* [17] procedure that is built upon Sundman transformation given below:

$$\sqrt{\mu}dt = rd\chi, \tag{3}$$

where χ is a "time-like" variable that is defined for all types of orbits. This allows the universal solution to be applicable without a-priori knowledge of the orbit's eccentricity (essentially the type of conic section). With this transformation, the map between time (t) and the "universal anomaly" (χ) is given by the universal Kepler's equation:

$$\sqrt{\mu}(t - t_0) = r_0 U_1(\alpha, \chi) + \sigma_0 U_2(\alpha, \chi) + U_3(\alpha, \chi), \tag{4}$$

where;

$$\alpha = \frac{1}{a}, \;\; \sigma = \frac{\mathbf{r} \cdot \mathbf{v}}{\sqrt{\mu}}. \tag{5}$$

and, where a is the semimajor axis and $U_n(\alpha, \chi)$ are the universal functions whose general form is given below:

$$U_n(\alpha, \chi) = \chi^n \left(\frac{1}{n!} - \frac{\alpha\chi^2}{(n+2)!} + \frac{(\alpha\chi^2)^2}{(n+4)!} - \frac{(\alpha\chi^2)^3}{(n+6)!} + \ldots \right). \tag{6}$$

Given t_0, t, $\mathbf{r}_0$, and $\mathbf{v}_0$, the universal Kepler's equation can be numerically solved to determine $\chi(t)$. Ultimately, $\mathbf{r}(t)$ and $\mathbf{v}(t)$ can be found in the following universal $F-G$ format:

$$\begin{aligned} \mathbf{r}(t) &= F(\chi)\mathbf{r}_0 + G(\chi)\mathbf{v}_0, \\ \mathbf{v}(t) &= \dot{F}(\chi)\mathbf{r}_0 + \dot{G}(\chi)\mathbf{v}_0, \end{aligned} \tag{7}$$

where; the Lagrange coefficients, F, G, $\dot{F}$ and $\dot{G}$ are:

$$\begin{aligned} F(\chi) &= 1 - \frac{U_2(\alpha, \chi)}{r_0}, \\ G(\chi) &= \frac{1}{\sqrt{\mu}}(r_0 U_1(\alpha, \chi) + \sigma_0 U_2(\alpha, \chi)), \\ \dot{F}(\chi) &= -\frac{\sqrt{\mu}}{r r_0} U_1(\alpha, \chi), \\ \dot{G}(\chi) &= 1 - \frac{U_2(\alpha, \chi)}{r}. \end{aligned} \tag{8}$$

Note that Eqs.7 represent a map between the initial conditions $(\mathbf{r}(t_0), \mathbf{v}(t_0))$ and the current states $(\mathbf{r}(t), \mathbf{v}(t))$. This is crucial for the MCMC-MOC approach described in Sec.IV.

III. Forward Monte Carlo (FMC)

In general, Monte Carlo is a broad class of computational algorithms that rely on repeated random sampling to obtain a particle representation of the state pdf at all times. For the initial uncertainty propagation problem, the initial pdf is discretized via random sampling and each sample is propagated forward in time through the system dynamics (Eq.2) to obtain the particle representation of uncertainty at future times. In our paper, we refer to this methodology as forward Monte Carlo (FMC).

Even though FMC is easy to implement and is the popular choice for propagation of initial uncertainty, there is scarcity of theoretical results pertaining to its performance, in particular its convergence rate. Some of the important questions regarding FMC for initial uncertainty propagation we are concerned with in this paper are the following:

1) The foundation of FMC is the law of large numbers (LLN). However, in terms of implementation, how "large" the initial ensemble must be in order to represent the state pdf sufficiently well at a future time?
2) Without even taking the dynamical system into account, how well do the forward propagated particles represent the state pdf at a future time?

In this paper, we show that for the two-body problem, the FMC approach is statistically equivalent to a newly developed MCMC-MOC method for uncertainty forecasting. Moreover, by construction the latter method builds a particle ensemble that is equivalent in measure to the true underlying system pdf at all times. As a result, it is unfortunately not possible to improve upon FMC particle results for the two-body problem.

IV. MCMC-MOC

In this section, we briefly introduce a recently developed Markov chain Monte Carlo (MCMC) based particle approach, combining the Markov chain Monte Carlo (MCMC) sampling technique ([18], [14]) with the method of characteristics for solving first order partial differential equations (PDEs), to propagation of initial uncertainty.

A. The Liouville Equation

Consider the nonlinear dynamical system as described in Sec. II-A (Eq.1). The time evolution of the state pdf, i.e. $W(t,\mathbf{x})$ is given by the stochastic Liouville equation, which is a first-order linear partial differential equation given as follows:

$$\frac{\partial}{\partial t}W(t,\mathbf{x}) = \mathscr{L}[W(t,\mathbf{x})], \tag{9}$$

where, $\mathscr{L}(\cdot)$ is the stochastic Liouville operator:

$$\mathscr{L}[W(t,\mathbf{x})] = -\left[W\,\nabla\cdot\mathbf{f} + \sum_{i=1}^{N} f_i \frac{\partial W}{\partial x_i}\right]. \tag{10}$$

On the RHS, the term $\nabla.\mathbf{f}$ is the divergence of the vector forcefield, that measures the strength of its source or sink at a given point in terms of a signed scalar. Alternatively, the divergence represents the volume density of the outward flux of a vector field from an infinitesimal volume around a given point. For example, if $\nabla.\mathbf{f}$ is a constant, then depending on its sign, the region of the vector field can be a source (expanding flow) or sink (contractive flow). In our recent work [19], we have determined that the performance of FMC can be evaluated based on whether the underlying system is divergence-free ($\nabla\cdot\mathbf{f} = \mathbf{0}$) or not. In the present context, the two-body problem has zero divergence (see Eq.2), whereby it can be shown [19] that the FMC approach will be statistically equivalent to the true measure of the system.

Also note that since the solution of Eq.9 must be a valid pdf at all times, appropriate boundary conditions must be satisfied: $\lim_{\mathbf{x}\to\infty} W(t,\mathbf{x}) = 0,\ \forall\ t \in [0,\infty)$. In addition, the solution must also satisfy the normality condition, i.e. $\int_{\Re^N} W(t,\mathbf{x})d\mathbf{x} = 1$ for all times $t \in [0,\infty)$. A particle method based on Markov chain Monte Carlo and the method of characteristics is presented next for solving the SLE.

B. Method of Characteristics

The method of characteristics is a powerful technique for solving first order quasi-linear partial differential equations (PDEs) of the following form:

$$\sum_{i=1}^{Q} g_i(z,u)\frac{\partial u}{\partial z_i} = h(\mathbf{z},u), \tag{11}$$

where, the unknown u is a function of $\mathbf{z} \in \Re^Q$. There exist special trajectories, called "characteristic curves" along with which the total-derivative of the unknown $u(\cdot)$ can be found. Along these characteristic lines, the above PDE can be converted to ODEs as follows [15].

$$\frac{dz_1}{g_1(z,u)} = \frac{dz_2}{g_2(z,u)} = \cdots = \frac{dz_Q}{g_Q(z,u)} = \frac{du}{h(z,u)}. \tag{12}$$

The above ODEs are called Lagrange-Charpit equations and they are valid only along the characteristic lines. Comparing the stochastic Liouville equation Eq.9 with the general quasi-linear PDE of Eq.11. We see that $z = [t,\mathbf{x}]'$ and the Lagrange-Charpit equations for the SLE become:

$$\frac{dx_1}{f_1(\mathbf{x},t)} = \cdots = \frac{dx_N}{f_N(\mathbf{x},t)} = \frac{dt}{1} = \frac{dW(t,\mathbf{x})}{-W(t,\mathbf{x})\nabla\cdot\mathbf{f}(t,\mathbf{x})}, \tag{13}$$

where, $\nabla\cdot\mathbf{f}(t,\mathbf{x})$ represents the divergence of the force field, thus giving us the time evolution of the pdf along a characteristic curve as:

$$\int_{t_0}^{t} \frac{dW(\tau,\mathbf{x}(\tau))}{W(\tau,\mathbf{x}(\tau))} = -\int_{t_0}^{t} \nabla\cdot\mathbf{f}(\tau,\mathbf{x}(\tau))d\tau. \tag{14}$$

Finally, carrying out the integration we get the current pdf as

$$W(t,\mathbf{x}(t)) = W_0[\mathbf{x}_0(\mathbf{x}(t))]\exp\left[-\int_{t_0}^{t}\nabla\cdot\mathbf{f}(\tau,\mathbf{x}(\tau))d\tau\right], \tag{15}$$

where, $W_0[\mathbf{x}_0(\mathbf{x}(t)]$ is the initial probability valued at the back-integrated point via its characteristic curve from the corresponding candidate sample at the current time.

A powerful feature of MCMC is that it does not require the knowledge of the target measure's normalization constant (η) in order to generate its particle representation. Moreover, MCMC can provide estimates of desired expectations without ever needing to compute the numerical value of η. MCMC samples are generated by building a Markov chain and allowing it to evolve through a period of initial transience, which is called "burn-in", and all samples generated during this period are discarded. Once the transience (or burn-in) is completed, the chain exhibits stationary behavior, whose distribution by design is the same as the target pdf, $\pi(\mathbf{x})$. In the current context, the target pdf is the state pdf at the desired time in future. Unfortunately, this pdf is unknown and therefore MCMC is combined with the method of characteristics (MOC) to generate its particle representation.

In our MCMC-MOC method, we utilize the Metropolis Hastings (MH) [13],[20] algorithm for generating the sample set, $\{X^i\}_{i=1}^{D} \sim \pi(\mathbf{x})$. The Markov chain is constructed by generating a candidate sample from a proposal distribution (a pdf that is easy to sample) at any desired time. The value of the state-pdf at this point at the current time, i.e. $W(t_f, \mathbf{x}_s)$ where $\mathbf{x}_s$ is the generated sample, is obtained via Eq.15 by first "back-propagating" the candidate through the system dynamics along a characteristic curve to obtain its corresponding initial condition $W_0[\mathbf{x}_0(\mathbf{x}_s(t))]$. Then, the SLE is forward propagated along the same characteristic to obtain the target density value at the candidate sample. The sample is then accepted or rejected based on its relative likelihood of belonging to the target measure. If a symmetric proposal pdf is used in the MH algorithm, the new sample is admitted into the chain with a probability of acceptance $\alpha = \min\left(1, \frac{W_s}{W_c}\right)$, where W_s and W_c are the values of the target pdf at the new sample and current chain location respectively. The ensemble constructed through this process provides a particle representation of the uncertainty at current time that is rigorously equivalent in measure to the current state-pdf [13], [18].

C. Divergence-free Nature of TBP

The SLE (Eq.9) for the two-body problem (Eq.2) can be written as:

$$\frac{\partial W}{\partial t} + \sum_{i=1}^{3}\left(v_i \frac{\partial W}{\partial x_i} - \frac{\mu x_i}{r^3}\frac{\partial W}{\partial v_i}\right) = -W[\nabla \cdot \mathbf{f}(t,\mathbf{x})]. \quad (16)$$

Recall that $\mathbf{r} \doteq [x_1, x_2, x_3]'$, $\mathbf{v} \doteq [v_1, v_2, v_3]'$ and $\mathbf{x} \doteq [\mathbf{r}; \mathbf{v}]$. As mentioned before, the TPB is divergence-free, i.e. $\nabla.\mathbf{f} = 0$. Following Eq.15, the solution of SLE along a characteristic line is simplified to

$$W(t, \mathbf{x}(t)) = W_0[\mathbf{x}_0(\mathbf{x}(t))]. \quad (17)$$

The above equation indicates that along a characteristic line, the pdf value remains invariant. In other words, as a particle starting from an initial condition evolves over the system manifold, only its location changes, not its "probability" or "weight" or "significance". This is highlighted by the above equation in that the state pdf at any candidate location at the current time maps into the initial pdf evaluated at the corresponding initial condition. In the example of the unperturbed two body problem, the mapping between the current and initial states is quite elegant and already given above in Sec.II via the universal $F-G$ solution. This contributes to the statistical equivalence between FMC and MCMC-MOC in the TBP. For more rigorous arguments, the reader is directed to Ref.[19].

V. Simulation Results

In this section, we provide the particle representation of the desired state pdf for the TBP at different times using the MCMC-MOC method described above. Statistical results are compared with forward Monte Carlo (FMC) simulation, in order to display their statistical equivalence.

A. MCMC-MOC

Let us consider the example of a geostationary orbit as the nominal orbit with the following parameters: $a = 1.5 \times 10^7 m$, $e = 0.2$, $i = 20°$, $\omega = \Omega = 0°$, $E_0 = 90°$ and $P = 5.0785hr$. Assume a multivariate Gaussian distribution $N(\mu_0, \sigma_0^2)$ as the initial pdf $W_0(\mathbf{x})$, where the $\mu_0 = [\mathbf{r}_0; \mathbf{v}_0]$ and σ_0^2 are given by

$$\begin{aligned}\mu_0 = [&-0.7500 \times 10^7 m;\, 1.2207 \times 10^7 m;\, 0.4443 \times 10^7 m;\\ &-5.1549 \times 10^3 m/s;\, 0 m/s;\, 0 m/s],\end{aligned} \quad (18)$$

$$\begin{aligned}\sigma_{A0}^2 &= \mathrm{diag}[10^6 m;\, 10^6 m;\, 10^6 m;\, 10^2 m/s;\, 10^2 m/s;\, 10^2 m/s]\\ \sigma_{B0}^2 &= \mathrm{diag}[10^{10} m;\, 10^{10} m;\, 10^{10} m;\, 50^2 m/s;\, 50^2 m/s;\, 50^2 m/s],\end{aligned} \quad (19)$$

where, two different initial covariances (low: σ_{A0}^2 and high: σ_{B0}^2) are used respectively. A series of particle representations of the time propagated state-pdfs are shown in Fig.1 obtained from the MCMC-MOC approach, demonstrating the expected deviations from Gaussianity.

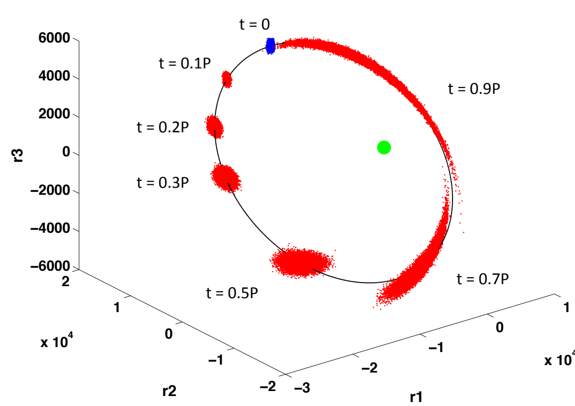

Fig. 1. MCMC Particle Representations of state-pdfs in $r_1 - r_2 - r_3$ space at various periods are given in red. Normal Orbit is shown in black line and initial uncertainty (σ_{B0}^2) is in blue. The results are scaled by 10^3m.

B. Adaptive Sampling

A crucial factor that affects the performance of MCMC-MOC is the effectiveness of the proposal density used for exploring the state-space. The main challenges we must face are: i) the state pdf resides in a 6-dimensional space, which entails a very large search-volume (dimensionality issue); and ii) the variance of the target pdf typically grows rapidly in a nonlinear manner. A standard MCMC sampler (e.g. using a fixed Gaussian proposal density) is unable to construct a Markov chain with good mixing in the face of dimensionality and nonlinearity as outlined above. Fig.2 gives an illustration of these difficulties. From Fig.2(a), we can see that the shape of the target pdf marginal (represented by a large amount of FMC points) in the $r_1 - r_2 - v_1$ space appears as a lathy section. Even worse, there exits a sharp curvature at one of the extremes near the tail region. Fig.2(b) shows that two proposed candidates (black square and red diamond) that almost coincide with each other at current time in the $r_1 - r_2 - r_3$ space end up in significantly different locations upon mapping back to the initial conditions. In fact, while the first candidate (black square) falls within the "high density region" of the initial pdf, the other (red diamond) lies deep in the tail. The reason is clearly visible in Fig.2(c), namely that the latter candidate falls outside the target pdf (shown approximately using the FMC ensemble) in the $r_1 - r_2 - v_1$ space and as a result, following Eq.17, falls in the outliers when mapped back to the initial time. Of-course, there is no way of knowing something like this would happen a-priori (i.e. without the benefit of the FMC representation). As a result, the standard Gaussian proposal is a poor choice and most of the candidates sampled from this proposal would be rejected, leading to an extremely slow exploration of the state-space.

It is possible to improve the acceptance rate by reducing the variance of the proposal. However, this can further reduce the exploration rate. There is need for a smarter "adaptive" MCMC sampler that attains a good mixing along with fast convergence. Most existing off-the-shelf adaptive MCMC samplers [21], [22], [23] are designed for specific forms of the target pdf and do not perform well in the current application.

Given the extremely complex structure of the target pdf in the current problem, we aimed to employ a proposal as close to the unknown target. This entails an unsymmetrical distribution, in which case the Hastings acceptance probability is given as

$$\alpha = \min\left(1, \frac{q(x_c|x_s)W_s}{q(x_s|x_c)W_c}\right). \tag{20}$$

The key idea is to use the "propagated proposal at the initial time (q_0)", as the proposal density at the current time. In essence, we simply employ the initial proposal, walking through it and propagating the generated candidate from q_0, at t_0, to its location at the current time along the characteristic curve, while being aware that the numerical value of the proposal density does not change due to the divergence free dynamics. Therefore, we are able to draw from an ideal proposal at the current time without ever knowing its exact functional form. Of course, this idea works only because the system is divergence free. Importantly, it obviates the quest for the ideal proposal at the current time in order to achieve good mixing, which is an extremely difficult task on account of the difficulties highlighted above (combination of a high dimensional search space with severe nonlinearity).

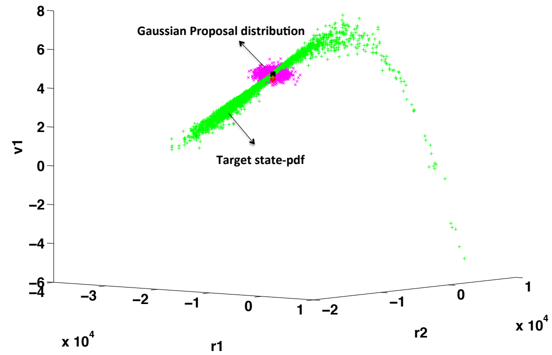

(a) Particle representation in $r_1 - r_2 - v_1$ space at $t = 0.6P$. Target state-pdf in green and proposal distribution in pink.

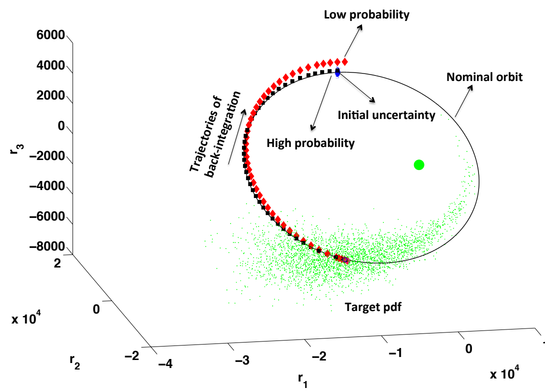

(b) The back-integration of two nearby points in $r_1 - r_2 - r_3$ space.

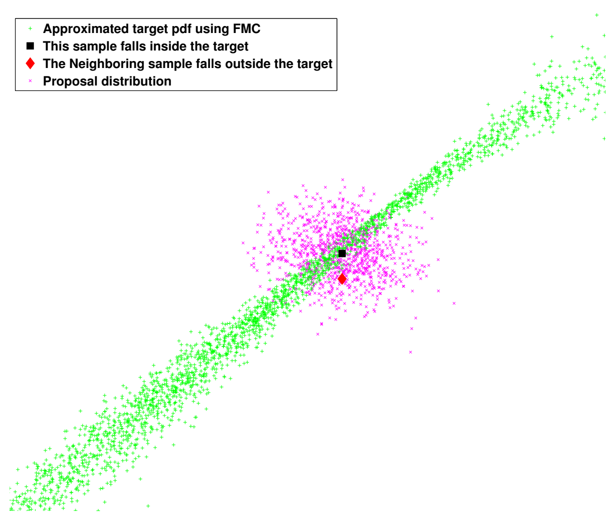

(c) The same neighboring points in $r_1 - r_2 - v_1$ space.

Fig. 2. An illustration of difficulties in MCMC-MOC sampling for the TBP.

C. FMC and MCMC-MOC

Here, we compare the statistics generated from the FMC and MCMC-MOC ensembles for the TBP. Two different cases of initial covariance: σ^2_{A0} (Case A) and σ^2_{B0} (Case B) with the same mean μ_0 are considered. Fig. 3 and 4 illustrate the mean and standard deviations at time $t = 0.6P$ as the number of points increases for both FMC (blue) and MCMC-MOC (red). The "baseline" (truth) is established by running an FMC simulation with 1 million samples, shown using a pink dotted line. The relative error in statistics computed from the MCMC-MOC method, with respect to the FMC "baseline" is given in Tables I and II. Also, Fig. 5 shows the evolution of statistics (mean and standard deviation) over time ($0.1P$, $0.2P$, $0.3P$, $0.5P$, $0.7P$ and $0.9P$) for both MCMC-MOC and FMC. As can be seen the relative error between statistics gained from MCMC-MOC ensemble compared with the FMC baseline is extremely small, which implies statistical equivalence between FMC and MCMC-MOC.

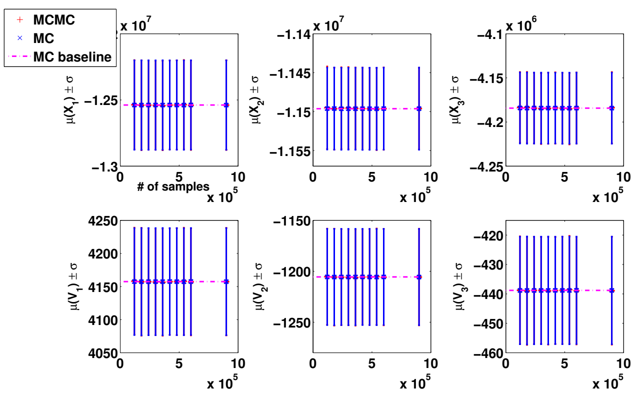

Fig. 3. Case A: Low Variance (σ^2_{A0}) Initial Uncertainty Propagation

Relative error of MCMC-MOC with FMC baseline	μ of MCMC-MOC (9×10^5)	σ of MCMC-MOC (9×10^5)
X_1	0.0057%	0.5%
X_2	0.0016%	0.5%
X_3	0.0123%	0.37%
V_1	0.0027%	0.48%
V_2	0.0061%	0.53%
V_3	0.0241%	0.43%

TABLE I
CASE A

It is important to underline some important characteristics for MCMC-MOC: (i) the shown particles in Fig.1 do not merely provide a visual feel for the state uncertainty at various times. These are equivalent in measure to the actual state pdf and can be used to directly compute expectations. (ii) it is no longer required to specify the "domain of solution". The developed method automatically samples points from where the pdf is "heavy"; (iii) The solution results

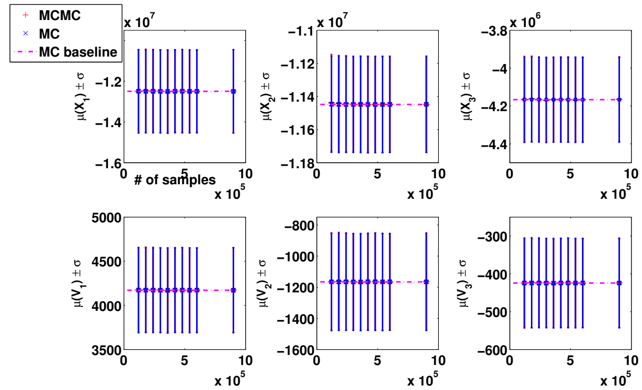

Fig. 4. Case B: High Variance (σ^2_{B0}) Initial Uncertainty Propagation

Relative error of MCMC-MOC with FMC baseline	μ of MCMC-MOC (9×10^5)	σ of MCMC-MOC (9×10^5)
X_1	0.07%	0.18%
X_2	0.004%	0.19%
X_3	0.05%	0.31%
V_1	0.05%	0.24%
V_2	0.09%	0.31%
V_3	0.08%	0.023%

TABLE II
CASE B

in not only the distribution of particles representing the state pdf, but also the value of the state-pdf at each of the particles. Rigorously speaking, MCMC-MOC should always be the benchmark instead of FMC. However, for systems with zero divergence, of which the TBP is an instance, they are equivalent according to above results.

VI. CONCLUSIONS

In this paper, we revisited the performance of traditional Monte Carlo algorithm for initial uncertainty propagation in the perturbation free two-body system. Its time varying statistics is compared with a recently developed MCMC based particle method. In this new approach, at any desired time in future, a Markov chain is constructed with the unknown state pdf as the target density. To evaluate the unknown target at a candidate sample, the stochastic Liouville equation is solved by the method of characteristics. The Metropolis acceptance criterion finally decides whether or not the candidate must be admitted into the particle representation of the state-pdf at the current time. By construction, it is equivalent in measure to the true propagated state-pdf. Numerical results in this paper confirm our theoretical results in [19] that for the TBP (divergence-free), the statistics of FMC and MCMC-MOC are coincident, which points to the fact the it is not possible to improve upon the slow convergence of FMC for initial uncertainty propagation in the unperturbed Keplerian dynamics.

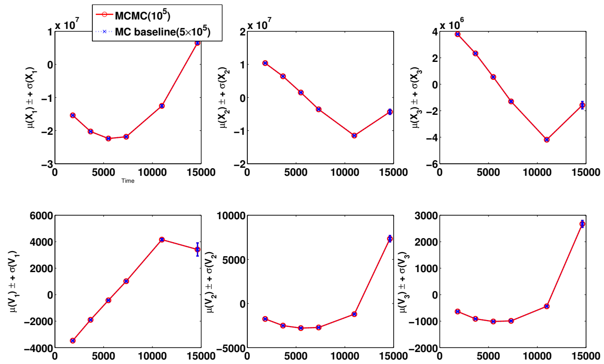

(a) Case A

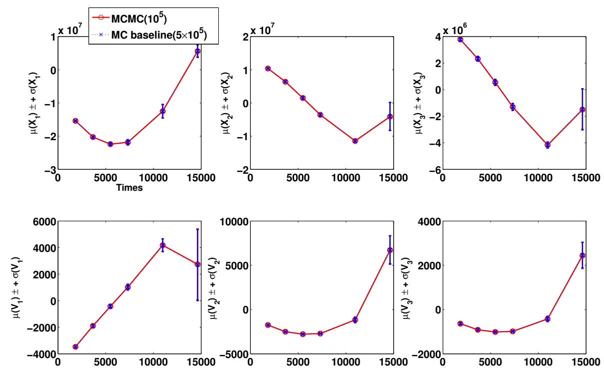

(b) Case B

Fig. 5. Time Propagation of Mean and Standard Deviation

REFERENCES

[1] H. Niederreiter, *Random Number Generation and Quasi-Monte Carlo Methods*. Society for Industrial and Applied Mathematics, 1992.

[2] R. E. Caflisch, "Monte carlo and quasi-monte carlo methods," *Acta Numerica*, vol. 7, pp. 1–49, Jan 1998.

[3] D. Giza, P. Singla, and M. Jah, "An approach for nonlinear uncertainty propagation: Application to orbital mechanics," in *AIAA Guidance, Navigation, and Control Conference, Chicago IL*, 2009.

[4] R. H. B. K. J. Demars and M. K. Jan, "A splitting gaussian mixturemethod for the propagation of uncertainty in orbital mechanics," *Spaceflight Mechanics*, vol. 140, 2011.

[5] T. S. Gabriel Terejanu, Puneet Singla and P. D. Scott, "Uncertainty propagation for nonlinear dynamic systems using gaussian mixture models," vol. 31, no. 6, pp. 1623–1633, 2008.

[6] B. A. Jones, A. Doostan, and G. H. Born, "Nonlinear Propagation of Orbit Uncertainty Using Non-Intrusive Polynomial Chaos," *Journal of Guidance Control Dynamics*, vol. 36, pp. 430–444, Mar. 2013.

[7] B. A. Jones and A. Doostan, "Satellite collision probability estimation using polynomial chaos expansions," *Advances in Space Research*, vol. 52, no. 11, pp. 1860 – 1875, 2013.

[8] Y. Sun and M. Kumar, "Numerical solution of high dimensional stationary fokkerplanck equations via tensor decomposition and chebyshev spectral differentiation," *Computers & Mathematics with Applications*, vol. 67, no. 10, pp. 1960 – 1977, 2014.

[9] ——, "Uncertainty propagation in orbital mechanics via tensor decomposition," *Celestial Mechanics and Dynamical Astronomy*, under review.

[10] K. Fujimoto, D. J. Scheeres, and K. T. Alfriend, "Analytical Nonlinear Propagation of Uncertainty in the Two-Body Problem," *Journal of Guidance Control Dynamics*, vol. 35, pp. 497–509, Mar. 2012.

[11] C. Yang and M. Kumar, "Beyond Monte Carlo for the Intial Uncertainty Propagation Problem," *Conference on Decision and Control*, 2014.

[12] M. Ehrendorfer, "The liouville equation and prediction of forecast skill," in *Predictability and Nonlinear Modelling in Natural Sciences and Economics*, J. Grasman and G. van Straten, Eds. Springer Netherlands, 1994, pp. 29–44.

[13] W. K. Hastings, "Monte Carlo sampling methods using Markov chains and their applications," *Biometrika*, vol. 57, no. 1, pp. 97–109, Apr. 1970.

[14] R. S. Gilks, W. R. and D. J. Spiegelhalter, *Markov Chain Monte Carlo in Practice (Chapman & Hall/CRC Interdisciplinary Statistics)*, 1st ed. Chapman and Hall/CRC, Dec. 1995.

[15] L. C. Evans, *Partial Differential Equations (Graduate Studies in Mathematics, V. 19) GSM/19*. American Mathematical Society, June 1998.

[16] H. Goldstein, C. P. Poole, and J. L. Safko, *Classical Mechanics (3rd Edition)*, 3rd ed. Addison-Wesley, June 2001.

[17] R. H. Battin, *An introduction to the mathematics and methods of astrodynamics*. Reston, VA: American Institute of Aeronautics and Astronautics, 1999.

[18] S. Meyn and R. L. Tweedie, *Markov Chains and Stochastic Stability*, 2nd ed. New York, NY, USA: Cambridge University Press, 2009.

[19] C. Yang, K. Buck, and M. Kumar, "An evaluation of monte carlo initial uncertainty propagation for divergence-free dynamics," *Phyics A, submitted*, 2015.

[20] S. Chib and E. Greenberg, "Understanding the metropolis-hastings algorithm," *The American Statistician*, vol. 49, no. 4, pp. 327–335, Nov. 1995.

[21] J. S. Rosenthal, "Optimal proposal distributions and adaptive mcmc," 2010.

[22] C. Andrieu and J. Thoms, "A tutorial on adaptive MCMC," *Statistics and Computing*, vol. 18, no. 4, pp. 343–373, 2008.

[23] H. Haario, E. Saksman, and J. Tamminen, "Componentwise adaptation for high dimensional mcmc," *Computational Statistics*, vol. 20, no. 2, pp. 265–273, 2005.